Nonclinical Study and Applicability of the Absorbed Dose Conversion Method With a Single Biodistribution Measurement for Targeted Alpha-Nuclide Therapy

Tetsuya Sakashita (sakashita.tetsuya@qst.go.jp)
National Institutes for Quantum and Radiological Science and Technology https://orcid.org/0000-0002-3357-8373

Shojiro Matsumoto
National Institutes for Quantum and Radiological Science and Technology

Shigeki Watanabe
National Institutes for Quantum and Radiological Science and Technology

Hirofumi Hanaoka
Gunma University Graduate School of Medicine

Yasuhiro Ohshima
National Institutes for Quantum and Radiological Science and Technology

Yoko Ikoma
National Institutes for Quantum and Radiological Science and Technology

Naoyuki Ukon
Fukushima Medical University

Ichiro Sasaki
National Institutes for Quantum and Radiological Science and Technology

Tatsuya Higashi
National Institutes for Quantum and Radiological Science and Technology

Tetsuya Higuchi
Gunma University Graduate School of Medicine

Yoshito Tsushima
Gunma University Graduate School of Medicine

Noriko S. Ishioka
National Institutes for Quantum and Radiological Science and Technology

---

Original research

Keywords: Targeted alpha-nuclide therapy, Dose conversion, Biodistribution, Pharmacokinetics, RAP

DOI: https://doi.org/10.21203/rs.3.rs-573658/v1

Version of Record: A version of this preprint was published at EJNMMI Physics on December 1st, 2021.
See the published version at https://doi.org/10.1186/s40658-021-00425-z.

Original research articles

Nonclinical study and applicability of the absorbed dose conversion method with a single biodistribution measurement for targeted alpha-nuclide therapy

Tetsuya Sakashita[1,*], Shojiro Matsumoto[1], Shigeki Watanabe[1], Hirofumi Hanaoka[2], Yasuhiro Ohshima[1], Yoko Ikoma[3], Naoyuki Ukon[4], Ichiro Sasaki[1], Tatsuya Higashi[3], Tetsuya Higuchi[5], Yoshito Tsushima[5], Noriko S. Ishioka[1]

[1]Quantum Beam Science Research Directorate, National Institutes for Quantum and Radiological Science and Technology, 1233 Watanuki-machi, Takasaki 370-1292, Japan

[2]Department of Bioimaging Information Analysis, Gunma University Graduate School of Medicine, 3-39-22 Showa, Maebashi 371-8511, Japan

[3]Department of Molecular Imaging and Theranostics, National Institutes for Quantum and Radiological Science and Technology, 4-9-1 Anagawa, Inage-ku, Chiba 263-8555, Japan

[4]Advanced Clinical Research Center, Fukushima Medical University, 1 Hikariga-oka, Fukushima 960-1295, Japan

[5]Department of Diagnostic Radiology and Nuclear Medicine, Gunma University Graduate School of Medicine, 3-39-22 Showa, Maebashi 371-8511, Japan

***Corresponding author:** Dr. Tetsuya Sakashita, Quantum Beam Science Research Directorate, National Institutes for Quantum and Radiological Science and Technology, 1233 Watanuki-machi, Takasaki 370-1292, Japan. Tel.: +81-27-346-9103; Fax: +81-27-346-9688. E-mail: sakashita.tetsuya@qst.go.jp

Abstract

Background: We recently reported a new absorbed dose conversion method, RAP (**RA**tio of **P**harmacokinetics), for ^{211}At-*meta*-astatobenzylguanidine (^{211}At-MABG) using a single biodistribution measurement (%ID/g). However, there were some mathematical ambiguities in determing the optimal timing of a single measurement of %ID/g. Thus, we aimed to mathematically reconstruct the RAP method and to examine the optimal timing of a single measurement.

Results: We derived a new formalism of the RAP dose conversion method at time *t* and investigated the new formalism's performance using a representative RAP coefficient with radioactive-decay weighting. Dose conversions by representative RAP coefficients predicted the true [^{211}At]MABG absorbed doses with an error of 10% or less. The inverses of the representative RAP coefficients plotted at 4 h post-injection, which was the optimal timing reported in the previous work, were very close to the new inverses of the RAP coefficients 4 h post-injection. Next, we acquired a formula to determine the optimal timing of a single measurement of %ID/g, assuming the one-compartment model for biological clearance. The behavior of the optimal timing was analyzed by radiolabeled compounds with physical half-lives of 7.2 h and 10 d on various biological clearance half-lives. Behavior maps of optimal timing showed a tendency to converge to a constant value

as the biological clearance half-life of a target increased. The areas of optimal timing for both compounds within a 5% or 10% prediction error were distributed around the optimal timing when the biological clearance half-life of a target was equal to that of the reference. Finally, an example of RAP dose conversion was demonstrated for [^{211}At]MABG.

Conclusions: The RAP dose conversion method renovated by the new formalism was able to estimate the [^{211}At]MABG absorbed dose using a similar pharmacokinetics, such as [^{131}I]MIBG. The present formalism revealed optimizing imaging time points on absorbed dose conversion between two radiopharmaceuticals. Further analysis and clinical data will be needed to elucidate the validity of a behavior map of the optimal timing of a single measurement for targeted alpha-nuclide therapy.

Keywords: Targeted alpha-nuclide therapy, Dose conversion, Biodistribution, Pharmacokinetics, RAP.

Background

^{211}At-*meta*-astatobenzylguanidine (^{211}At-MABG) is a potential nuclear medicine for targeted alpha-nuclide therapy (TAT). ^{131}I-*meta*-iodobenzylguanidine (^{131}I-MIBG) therapy has also been used for the palliative treatment of patients with malignant paraganglioma and phaeochromocytoma [1]. Some patients with poor prognoses might undergo ^{211}At-MABG treatment for remission. In ^{131}I-MIBG therapy, diagnostic imaging by ^{131}I-scintigraphy and/or SPECT during ^{131}I-MIBG treatment would be performed occasionally as part of follow-up care, because such imaging is of clinical prognostic value. Predicting the organ or tumor tissue absorbed dose of such patients in ^{211}At-MABG treatment using ^{131}I-MIBG image data would be useful for planning ^{211}At-MABG therapy. Therefore, it is important to develop methods for estimating ^{211}At-MABG doses using ^{131}I-MIBG biodistribution data.

At present, one of issues in systemic radiopharmaceutical therapy or TAT is optimizing imaging time points [2]. The previous work of Madsen et al. [3] revealed a single-time to estimate the total integrated activity and absorbed dose to within 10% accuracy. Recently, we reported a novel dose conversion method, RAP (**RA**tio of **P**harmacokinetics), using biodistribution data, namely the percent injected dose/g (%ID/g) [4]. In that study, we extended optimizing imaging time points on absorbed dose

conversion between two radiopharmaceuticals, and demonstrated that the RAP dose conversion method could estimate ^{211}At-MABG absorbed doses from a single measurement of %ID/g and the pharmacokinetics of ^{131}I-MIBG in a 24 h evaluation period. However, at that time we were unable to present a sufficient mathematical approach for the timing of a single measurement of %ID/g. Moreover, only proportional relations formed the mathematical basis of the RAP method, resulting in some mathematical ambiguities. Therefore, we aimed to describe the RAP method mathematically without proportional relations and to examine the timing of a single measurement of %ID/g.

In the present paper, we proposed a novel formula to estimate the optimal timing of a single measurement of %ID/g and analyzed the behavior of the optimal timing depending on the biological pharmacokinetic parameters. Also, we used two other sets with a short evaluation period (6 h): ^{77}Br-*meta*-bromobenzylguanidine (^{77}Br-MBBG) and ^{125}I-*meta*-iodobenzylguanidine (^{125}I-MIBG) to examine the performance of the RAP conversion. Moreover, we present an example of RAP dose conversion using a behavior map of the optimal timing of a single measurement of %ID/g.

Materials and Methods

Simulation datasets

On time-series of biodistribution profiles in our previous Monte Carlo simulation work on ^{211}At-MABG, ^{131}I-MIBG, ^{77}Br-MBBG, and ^{125}I-MIBG, we used a total of 8,000 simulation (virtual experiment) datasets [4]. In the present study, we applied a median of 200 simulation datasets at each organ or tumor tissue. The simulation was carried out based on the biodistribution profiles of three reports at several time points of seven organs (heart, liver, kidney, intestine, blood, adrenals, stomach) and tumor tissue [3, 4, 5]. One of these reports, by Vaidyanathan et al., reported the biodistributions of ^{211}At-MABG and ^{131}I-MIBG in nude mice with SK-N-SH human neuroblastoma xenografts [5]. In the second, by Ohshima et al. [6], a rat PC12 pheochromocytoma model was used to examine the antitumor effects of ^{211}At-MABG. The third report, by Watanabe et al. [7], analyzed the biodistributions of ^{77}Br-MBBG and ^{125}I-MIBG using PC12 xenografts. We have labeled the simulated biodistribution datasets created from these previous reports as [^{211}At]MABG [5], [^{131}I]MIBG [5], [^{211}At]MABG [6], [^{77}Br]MBBG [7], and [^{125}I]MIBG [7], respectively. Their experimental conditions are shown in Table 1.

New formalism of RAP method at time *t*

In our previous work, we could not present a sufficient mathematical approach to the

timing of a single measurement. The mathematical basis of the RAP method was the proportional relation as follows:

$$D\ \left(^{211}At\right) \propto D\ \left(^{131}I \rightarrow {}^{211}At\right) \times \frac{1}{\frac{\%\mathrm{ID/g}\ \left(^{131}I\right)}{\%\mathrm{ID/g}\ \left(^{211}At\right)}}\ , \quad (1)$$

where, $D\ (^{211}At)$ is the absorbed dose of ^{211}At, $D\ (^{131}I \rightarrow ^{211}At)$ means the absorbed dose conversion using the exchange of the physical half-life (HL) in the activity concentration, and $\frac{1}{\frac{\%\mathrm{ID/g}\ \left(^{131}I\right)}{\%\mathrm{ID/g}\ \left(^{211}At\right)}}$ is the RAP coefficient defined in the previous work [4]. There were some mathematical ambiguities.

Here, we show a new derivation method for the RAP formula based on the activity concentration (kBq/g) of an organ or tumor tissue, $C\ (t)$. In the previous work, $C\ (t)$ was expressed using the two-biological-compartments model for normal organs except adrenals:

$$C(t) = C_0 exp\left(-\frac{ln(2)}{T_p}t\right)\left\{f exp(-\frac{ln(2)}{T_{b1}}t) + (1-f) exp(-\frac{ln(2)}{T_{b2}}t)\right\}, \quad (2)$$

where $C(t)$ is the activity concentration for the normal organ at time (sec) t post-injection, C_0 is the initial activity concentration, T_p is the physical HL time (sec), and f and $(1-f)$ are the fractions of the two biological compartments on clearance. T_{b1} and T_{b2} are the corresponding HL times (sec) for fast and slow biological clearances, respectively. Or, in the case of adrenals and tumor tissue, the following one-compartment equation was used:

$$C(t) = C_0\left(1 - exp(-\frac{ln(2)}{T_{up}}t)\right) exp(-\frac{ln(2)}{T_p}t)\ \ exp(-\frac{ln(2)}{T_{b1}}t),$$

(3)

where T_{up} is the HL time of uptake (sec).

In this study, we re-expressed activity concentration equations (2) and (3) as follows using injected dose concentration IDC_0 (Bq/ml) and %ID/g (t) at time (sec) t post-injection:

$$C(t) = IDC_0 exp(-\frac{ln(2)}{T_p}t) \ (\%\mathrm{ID/g}) \ (t) \quad , \tag{4}$$

where, in the previous simulation work, we assumed an injection with 100 kBq of ^{211}At-MABG in 100 μL of PBS into a tail vein and around 1 MBq as the total activity of a mouse. Next, we applied this equation to two radiolabeled compounds, A_1 and A_2.

$$C\_A_1(t) = IDC_0\_A_1 \ exp(-\frac{ln(2)}{T_{pA_1}}t) \ (\%\mathrm{ID/g})_{A_1}(t) \ and \tag{4-1}$$

$$C\_A_2(t) = IDC_0\_A_2 exp(-\frac{ln(2)}{T_{pA_2}}t) \ (\%\mathrm{ID/g})_{A_2}(t). \tag{4-2}$$

By dividing and transforming both sides of the (4-1) and (4-2) equations, we described the following new derivative relation for the RAP formalism:

$$C\_A_1(t) = C\_A_2(t) \frac{IDC_0\_A_1}{IDC_0\_A_2} \frac{exp(-\frac{ln(2)}{T_{pA_1}}t)}{exp(-\frac{ln(2)}{T_{pA_2}}t)} \frac{1}{\frac{(\%\mathrm{ID/g})_{A_2}(t)}{(\%\mathrm{ID/g})_{A_1}(t)}} \ . \tag{5}$$

Here, $\frac{1}{\frac{(\%\mathrm{ID/g})_{A_2}(t)}{(\%\mathrm{ID/g})_{A_1}(t)}}$ is the RAP coefficient at t. We assumed IDC_0 to 1 MBq/ml for both radiolabeled compounds A_1 and A_2 and set $IDC_0\_A_1$ / $IDC_0\_A_2$ to 1. If the injected dose concentration is different, we recommend normalizing it to 1 MBq/ml and multiplying the required concentration x times (MBq/ml), to the calculated result. To calculate a time

integration activity concentration (TIAC) (Bq-h/g) of radiolabeled compounds A_1 and A_2, we numerically integrated equation (5) with a 1 h interval.

The absorbed radiation dose (Gy), D, for normal or tumor tissue was calculated according to the following modified MIRD formalism:

$$D = 1000 \cdot TIAC \cdot E \cdot F \cdot P, \quad (6)$$

where the energy emitted by ^{211}At, E, is assumed to be solely from the alpha disintegrations, corresponding to 6.9 MeV / Bq-s [8]. The absorbed fraction, F, is set to 1, since it is assumed that all energy emitted by ^{211}At is absorbed by the source tissue or organ. P is the coefficient for converting from g to kg, 1000. Finally, the absorbed dose (J/kg = Gy) was calculated using the relation of 1.602 10^{-13} (J/MeV).

Framework for practical use of the RAP dose conversion

In the present work, we set radiolabeled compound A_2, which has a well-known biological kinetics, as a reference, and radiolabeled compound A_1 as a target with unknown biological kinetics. Our goal is to convert from the absorbed dose of A_2 to that of A_1. Integrating equation (5) leads to a TIAC (Bq-h/g) of A_1, but, in the case of unknown biological kinetics of A_1, integration would be difficult. On the other hand, the physical part of equation (5), that is, equation (5) except for the RAP coefficient, could be easily

integrated if the pharmacokinetics of A_2 is well known. Here, it should be noted that a single measurement of %ID/g has been used to demonstrate successful RAP dose conversion [4]. In short, we needed to work on simplifying the integration of the RAP coefficients, and used simulation datasets from the previous work to achieve that.

In the first attempt, the analysis of RAP coefficients, we numerically integrated the physical part of equation (5) except for the RAP coefficient. We also calculated the mean value of the target's radioactive-decay weighted RAP coefficients during the evaluation period, representative RAP coefficient. TIACs were obtained by multiplying the integral value of the physical part by the representative RAP coefficient. Finally, absorbed doses were estimated using equation (6). We labeled the absorbed dose based on the TIACs that were considered the physical part of the integration as "with HL", and that considered TIACs multiplied by the representative RAP coefficient as "with HL + RAP".

In the next attempt, the generalization of the RAP method, we acquired the formula for the optimal timing of a single measurement of %ID/g, assuming the one-compartment model for biological clearance. The TIAC of A_1, $TIAC\_A_1$, and that of A_2, $TIAC\_A_2$, with HL were expressed by the following equations, respectively:

$$TIAC\_A_1 = \frac{A_0\_A_1}{-\ln 2\left(\frac{1}{T_{pA_1}}+\frac{1}{T_{bA_1}}\right)}\left[\exp\left(-\ln 2\left(\frac{1}{T_{pA_1}}+\frac{1}{T_{bA_1}}\right)t\right)\right]_{t_0}^{t_1}, \quad (7a)$$

$$TIAC\_A_2\ with\ HL = \frac{A_0\_A_2}{-\ln 2\left(\frac{1}{T_{pA_1}}+\frac{1}{T_{bA_2}}\right)}\left[\exp\left(-\ln 2\left(\frac{1}{T_{pA_1}}+\frac{1}{T_{bA_2}}\right)t\right)\right]_{t_0}^{t_1}, \quad (7b)$$

where $A_0\_A_1$ and $A_0\_A_1$ are the initial activity concentrations, and T_{bA1} and T_{bA2} are HLs for biological clearances of radiolabeled compounds A_1 and A_2, respectively. t_0 and t_1 are the start and end times of the evaluation period. Here, the optimal timing of a single measurement of %ID/g should satisfy the following relation because of equations (1):

$$\text{RAP coefficient} = \frac{TIAC\_A_1}{TIAC\_A_2\ with\ HL}. \quad (8)$$

Then, the optimal timing, *Opt_t*, was solved as follows:

$$Opt\_t = \frac{1}{-\ln 2\left(\frac{1}{T_{bA_1}}-\frac{1}{T_{bA_2}}\right)}\ln\frac{\frac{1}{\frac{1}{T_{pA_1}}+\frac{1}{T_{bA_1}}}\left[\exp\left(-\ln 2\left(\frac{1}{T_{pA_1}}+\frac{1}{T_{bA_1}}\right)t\right)\right]_{t_0}^{t_1}}{\frac{1}{\frac{1}{T_{pA_1}}+\frac{1}{T_{bA_2}}}\left[\exp\left(-\ln 2\left(\frac{1}{T_{pA_1}}+\frac{1}{T_{bA_2}}\right)t\right)\right]_{t_0}^{t_1}}, \quad (9)$$

Finally, we present an example of dose conversion by the RAP method using a mathematical formula for the optimal timing, equation (9), for a single measurement of %ID/g.

Results

Analysis of the RAP coefficients

For the analysis of the RAP coefficients, we prepared the converted absorbed doses of [^{131}I]MIBG [5], [^{211}At]MABG [6], [^{125}I]MIBG [7], and [^{77}Br]MBBG [7] as references and the true absorbed dose of [^{211}At]MABG [5] as a target, using the simulation datasets of the previous work [4]. Here, for example, the converted absorbed dose of [^{131}I]MIBG [5] indicates the absorbed dose of an organ or tumor tissue when alpha rays derived from ^{211}At were emitted by the number of radioactive decays of ^{131}I. To investigate the relation between the RAP coefficient and the optimal timing of a single measurement of %ID/g, we produced a new derivative relation for RAP formalism, equation (5). In our first attempt at equation (5), we employed radioactive-decay weighting for the RAP coefficients at t and calculated the representative RAP coefficient for the evaluation period. We multiplied the representative RAP coefficient by the physical HL-corrected TIAC of a reference. Then, we calculated absorbed doses based on the physical HL-corrected TIAC, that is, “with HL”, and the physical HL-corrected and RAP-converted TIAC, which we labeled “with HL + RAP”.

Figure 1 shows the converted absorbed doses of the references, the “with HL”-corrected ones, the “with HL + RAP” ones, and the true absorbed dose of the [^{211}At]MABG [5] target. Most “with HL + RAP” converted absorbed doses were closer to the true absorbed dose of [^{211}At]MABG than the “with HL” ones. Average percent

differences between converted and true absorbed [^{211}At]MABG_1996[5] doses were -23% in “with HL” of [^{131}I]MIBG [5] and 7% in “with HL + RAP”. Similarly, those of [^{211}At]MABG [6] were 112% and -7%, those of [^{125}I]MIBG [7] were 53% and -2%, and those of [^{77}Br]MBBG [7] were 74% and -2% (Table 2). These results showed that the dose conversions by the representative RAP coefficients were able to predict the true value with an error of 10% or less.

To examine the ratio in %ID/g of a reference to a target, we plotted the inverse of the RAP coefficient (Figure 2). The inverses of the RAP coefficients at *t* changed over time in the seven organs and the tumor tissue. The inverses of the representative RAP coefficients were plotted at 4 h post-injection, which was the optimal timing reported in the previous work [4]. As a result, we found that the inverse values of RAP coefficients 4 h post-injection and the representative RAP coefficient were very close to each other. Taken together, these results suggest that the new RAP coefficients at 4 h post-injection corresponded to the RAP coefficients in the previous work.

Behavior of optimal timing of a single biodistribution measurement

The representative RAP coefficient needs to be based on the detailed kinetics of radiolabeled compound A_1 as a target, but we could estimate the ^{211}At-MABG absorbed

dose from a single biodistribution measurement. We should return to the origin of the RAP dose conversion, which is equation (8). Therefore, an optimal timing needs to satisfy the relation in equation (8). Assuming the one-compartment model for biological clearance, we calculated TIACs of A_1 and A_2 analytically, and the optimal timing was solved by equation (9). Interestingly, equation (9) did not include the physical HL time of radiolabeled compound A_2. Using this equation, we investigated the behavior of the optimal timing of a single measurement of %ID/g.

The behavior of an optimal timing on ^{211}At-labeled A_1 was estimated depending on the HLs of the biological clearance of a target, T_{bA1}, from 0 to 100 h and the HLs of the biological clearance of a reference, T_{bA2}, of 5, 10, 15, 20, 25, and 50 h (Figure 3). Here, we set the end time of the evaluation period to 72 h, which was 10 times the HL of ^{211}At. In addition, we plotted 0.9, 0.95, 1.05, and 1.1 times TIACs of A_1 in order to understand the area of optimal timing where the absorbed dose could be estimated within a 5% or 10% prediction error. As shown in figure 3, the optimal timing tended to converge to a constant value as T_{bA1} increased. Interestingly, all optimal timing values were acceptable when T_{bA1} was equal to T_{bA2}. The area of an optimal timing within a 5% or 10% prediction error was distributed around the intersection where the curve of optimal timing agreed with the line where T_{bA1} was equal to T_{bA2}.

Figure 4 shows the behavior of an optimal timing on A_1 with a physical HL of 10 d, e.g., ^{225}Ac, depending on T_{bA1} from 0 to 250 h and T_{bA2} of 25, 50, 100, and 200 h. Here, we set the end time of the evaluation period to 2,400 h. The optimal timing also tended to converge to a constant value as T_{bA1} increased, and the convergence value was larger than that of ^{211}At. The area of optimal timing within a 5% or 10% prediction error was also distributed around the intersection where the curve of optimal timing agreed with the line where T_{bA1} was equal to T_{bA2}. In addition, an enlarged view of the behavior map at 25 h T_{bA2} shows that the behavior was almost the same as that for ^{211}At except for a different convergence value (Figure 5a). Moreover, short HLs of biological clearance in T_{bA1} and T_{bA2} displayed short optimal timing (Figure 5b). These results suggest that the area of optimal timing depended on both T_{bA1} and T_{bA2}, and that the convergence value of the optimal timing was controlled by the physical HL time of radiolabeled compound A_1.

Example of RAP dose conversion using optimal timing of a single biodistribution measurement.

Analysis of RAP coefficients and of a behavior map of the optimal timing of a single measurement of %ID/g confirmed the practical applicationof the RAP method. Here, we present a case of the heart in [^{131}I]MIBG [5] as a reference and [^{211}At]MABG [5] as a

target, using the simulation datasets from the previous work [4].

First, we plotted values converted to logarithms of [^{131}I]MIBG [5] corrected by the physical half-life of ^{131}I and fitted by the linear function, which was "a t + b" (Figure 6a). The fitted function was -0.1006 t + 4.7768 (R^2 = 0.926). From this relation, we estimated that the HL of the biological clearance of a reference, T_{bA2}, was 6.89 h. Next, we drew the behavior map of the optimal timing on A_1 labeled with ^{211}At and with T_{bA2} of 6.9 h (Figure 6b). From the behavior map, we decided that 5 h of optimal timing, assuming the HL of the biological clearance of a target, T_{bA1}, was close to that of T_{bA2}. We calculated the inverse of the RAP coefficient from the values of %ID/g in simulation datasets of radiolabeled compound A_1 and radiolabeled compound A_2, which was 0.76. Finally, we estimated an absorbed dose of 3.3 Gy of [^{211}At]MABG [5], by multiplying the RAP coefficient by that of the physical HL-corrected absorbed dose, 2.7 Gy, which is a numerical integration of the physical part of equation (5) (Figure 6c). The difference between the RAP-converted absorbed dose and a true [^{211}At]MABG_1996[5] absorbed dose was 7%, which was superior to the 10% prediction error obtained by the representative RAP coefficient in Table 2. This result suggests that the present RAP dose conversion method is practical enough to use.

Discussion

In this study, we focused on the mathematical ambiguities we encountered in our derivation of RAP coefficients in our previous work. We aimed to describe the RAP method mathematically without proportional relations and to examine the timing of a single biodistribution measurement (%ID/g). Here, we proposed a novel formula to estimate the optimal timing of a single measurement of %ID/g. Analysis of the behavior on the optimal timing revealed that the physical HL time of a target radiolabeled compound depended on the biological clearances of both the target and reference radiolabeled compounds. Finally, we presented an example of a practical use of RAP dose conversion.

A behavior map of an optimal timing on a single measurement of %ID/g might lead to several important strategies for RAP dose conversion. The first strategy involves a selection of a long biological clearance of a reference against a target with short and long physical HLs. If we could select a long biological clearance of a reference, we would have a broad window for optimal timing of a single biodistribution measurement (Figures 3 and 4). For example, in the case of a target with 10 d physical HL, over 25 h of the biological clearance HLs of a target and a reference could make an almost 1 h window for optimal timing (figure 5a). The second is the operation of the short biological

clearance HLs of a target and of a reference as shown in figure 5b. Even with a long physical HL, e.g., ^{225}Ac, it might be possible to obtain the RAP coefficient within a feasible and short time by this operation, although it would be limited to a case of appropriate drug delivery. For example, the HLs of the biological clearance of nuclear medicine using the prostate-specific membrane antigen (PSMA) in animal studies were around 1 h [9]. A behavior map of an optimal timing might make it possible to present an appropriate imaging plan with a single measurement biodistribution for nuclear medicines that are difficult to measure multiple times.

The optimal timing equation (9) could have an infinite end time of the evaluation period. If a one-compartment assumption for biological clearance holds for infinite time, the optimal timing equation could be transformed as follows:

$$Opt\_t = \frac{1}{-\ln 2\left(\frac{1}{T_{bA_1}}-\frac{1}{T_{bA_2}}\right)} \ln \frac{\frac{1}{T_{pA_1}}+\frac{1}{T_{bA_2}}}{\frac{1}{T_{pA_1}}+\frac{1}{T_{bA_1}}}, \quad (10)$$

where Opt_t is an optimal timing, T_{pA1} is the physical HL of a target, T_{bA1} is the biological clearance HL of a target, and T_{bA2} is the biological clearance HL of a reference. However, verifiable data are rarely available for infinite time. In this paper, we proposed equation (9) of the optimal timing with a limited evaluation period, so that we could apply it even when the activity concentration data were available for only a short evaluation period. In fact, this was the case with our simulations of all datasets (Table 1). In addition, an optimal

timing formulated by equation (9) has limited application because of an assumption of the one-compartment model for biological clearance. This one-compartment assumption does not hold in the early stages of the evaluation period, when the uptake of radiolabeled compounds continues for a long time, as in equation (3). Therefore, in this case it is necessary to adjust the start time of the evaluation. This is a future issue.

We should note that RAP dose conversion using a behavior map did not require difficult formulas and techniques. We would need only the physical HL correction, linear fitting, the calculations of equation (9), and a numerical integration such as a trapezoidal quadrature. For example, most researchers would use absorbed dose estimation software, e.g., Organ Level INternal Dose Assessment/EXponential Modeling (OLINDA/EXM) (Vanderbilt University, Nashville, TN, USA) [10]. Using these programs, users estimate the time activity curve (TAC) of a radionuclide-labeled compound fitted by the exponential functions. The value per unit weight of the TAC corresponds to *C(t)* in the present equation (4) and input for the example as shown in figure 6, indicating the feasibility of RAP dose conversion. OLINDA/EXM users could also use RAP dose conversion.

Unfortunately, clinical RAP coefficient information does not exist, and consideration of the RAP coefficient in animal biodistribution studies is currently limited.

Also, an approximation of the one-compartment model applied to a behavior map of an optimal timing might create limitations in use. However, even in the biological clearance of [^{131}I]MIBG [5] with a two-compartment phase [11], the RAP dose conversion displayed superior prediction error of less than 10%. The approach presented in a behavior map of an optimal timing on a single biodistribution measurement might provide useful information for the treatment planning of ^{211}At-MABG therapy or TAT. Taken together, these results underscore the importance of developing the RAP dose conversion method for nonclinical and clinical future studies.

Conclusions

The RAP dose conversion method renovated by the new formalism was able to estimate the [^{211}At]MABG absorbed dose using the pharmacokinetics of [^{131}I]MIBG through the use of a behavior map of an optimal timing of a single biodistribution measurement. The present formalism revealed optimizing imaging time points on absorbed dose conversion between two radiopharmaceuticals. Further analysis and clinical data will be needed to elucidate the validity of a behavior map of an optimal timing of a single measurement for TAT.

Abbreviations

HL: Half-life;

%ID/g: Percent injected dose per gram;

RAP: RAtio of Pharmacokinetics;

TIAC: Time integration activity concentration;

MIRD: Medical internal radiation dose

Acknowledgements

Not applicable.

Authors' contributions

Conceptualization: TS; Data validation and curation: SW, HH, YO, IS; Experimental design: TS, YI, NU, TH, YT; Modeling and analysis: TS, SM; Scientific writing: TS, SM, HH, TH; Securance of funding: NSI. All authors read and approved the final manuscript.

Funding

This work was supported in part by a KAKENHI grant (JP19H04296) from the Japan Society for the Promotion of Science to Dr. N. Suzui.

Availability of data and materials

The datasets used and/or analyzed in the present study are available from the corresponding author on reasonable request.

Declarations

Ethics approval and consent to participate

This article does not contain any studies with animals and human participants performed by any of the authors.

Consent for publication

Not applicable.

Competing interests

The authors declare that they have no competing interests.

Author details

[1]Quantum Beam Science Research Directorate, National Institutes for Quantum and

Radiological Science and Technology, 1233 Watanuki-machi, Takasaki 370-1292, Japan

[2]Department of Bioimaging Information Analysis, Gunma University Graduate School of Medicine, 3-39-22 Showa, Maebashi 371-8511, Japan

[3]Department of Molecular Imaging and Theranostics, National Institutes for Quantum and Radiological Science and Technology, 4-9-1 Anagawa, Inage-ku, Chiba 263-8555, Japan

[4]Advanced Clinical Research Center, Fukushima Medical University, 1 Hikariga-oka, Fukushima 960-1295, Japan

[5]Department of Diagnostic Radiology and Nuclear Medicine, Gunma University Graduate School of Medicine, 3-39-22 Showa, Maebashi 371-8511, Japan

References

1. van Hulsteijn LT, Niemeijer ND, Dekkers OM, Corssmit EP. ^{131}I-MIBG therapy for malignant paraganglioma and phaeochromocytoma: systematic review and meta-analysis. Clin Endocrinol. 2014;80:487-501.

2. Roncali E, Capala J, Benedict SH, Akabani G, Bednarz B, Bhadrasain V, Bolch WE, Buchsbaum J, Clarke BN, Coleman N, Dewaraja YK, Frey EC, Ghaly M, Grudzinski J, Hobbs RF, Howell RW, Humm JL, Kunos C, Larson SM, Lin FI, Madsen MT, Mirzadeh

S, Morse DL, Pryma DA, Sgouros G, James SS, Wahl RL, Xiao Y, Zanzonico PB, Zukotynski K. Overview of the First NRG-NCI Workshop on Dosimetry of Systemic Radiopharmaceutical Therapy (RPT). J Nucl Med. 2020; doi: 10.2967/jnumed.120.255547.

3. Madsen MT, Menda Y, O'Dorisio TM, O'Dorisio MS. Technical Note: Single time point dose estimate for exponential clearance. Med Phys. 2018; 45: 2318–24.

4. Sakashita T, Watanabe S, Hanaoka H, Ohshima Y, Ikoma Y, Ukon N, Sasaki I, Higashi T, Higuchi T, Tsushima Y, Ishioka SN. Absorbed dose simulation of *meta*-^{211}At-astato-benzylguanidine using pharmacokinetics of ^{131}I-MIBG and a novel dose conversion method, RAP. Ann Nucl Med. 2021;35:121-31.

5. Vaidyanathan G, Friedman HS, Keir ST, Zalutsky MR. Evaluation of *meta*-[^{211}At]astatobenzylguanidine in an athymic mouse human neuroblastoma xenograft model. Nucl Med Biol. 1996;23:851-6.

6. Ohshima Y, Sudo H, Watanabe S, Nagatsu K, Tsuji AB, Sakashita T, Ito YM, Yoshinaga K, Higashi T, Ishioka NS. Antitumor effects of radionuclide treatment using α-emitting *meta*-^{211}At-astato-benzylguanidine in a PC12 pheochromocytoma model. Eur J Nucl Med Mol Imaging. 2018;45:999-1010.

7. Watanabe S, Hanaoka H, Liang JX, Iida Y, Endo K, Ishioka NS. PET imaging of

norepinephrine transporter-expressing tumors using ^{76}Br-*meta*-bromobenzylguanidine. J Nucl Med. 2010;51:1472-9.

8. Spetz J, Rudqvist N, Forssell-Aronsson E. Biodistribution and dosimetry of free ^{211}At, ^{125}I- and ^{131}I- in rats. Cancer Biother Radiopharm. 2013;28:657-64.

9. Christoph AU, Martina B, Raffaella MS, Andreas T, Roger S, Nicholas PM, Cristina M. ^{44}Sc-PSMA-617 for radiotheragnostics in tandem with ^{177}Lu-PSMA-617-preclinical investigations in comparison with ^{68}Ga-PSMA-11 and ^{68}Ga-PSMA-617. EJNMMI Res. 2017;7(1):9.

10. Stabin MG, Sparks RB, Crowe E. OLINDA/EXM: the second-generation personal computer software for internal dose assessment in nuclear medicine. J Nucl Med. 2005;46:1023–7.

11. Hjornevik T, Martinsen AC, Hagve SE, Andersen MW, Mørk AC, Fjeld JG, Ruud E. Experiences from introducing standardized high dose ^{131}I-mIBG treatment of children with refractory neuroblastoma: differences in effective dose to patients and exposure to caregivers. J Nucl Med Radiat Ther. 2015;6:6.

Figure legends

Fig. 1 Comparison between converted absorbed doses of [^{131}I]MIBG [5], [^{211}At]MABG [6], [^{125}I]MIBG [7], and [^{77}Br]MBBG [7] and the true target absorbed dose of [^{211}At]MABG [5]. (a) Converted absorbed doses from [^{131}I]MIBG [5] as a reference, and absorbed dose of [^{211}At]MABG [5] as a true target. [^{131}I]MIBG [5] indicates the absorbed dose of an organ or tumor tissue when alpha rays derived from ^{211}At were emitted by the number of radioactive decays of ^{131}I. “with half-life (HL)” shows a converted absorbed dose of [^{131}I]MIBG [5] corrected by the physical half-life of ^{131}I and radioactively decayed with the physical half-life of ^{211}At, indicating the physical part of equation (5). ″with HL + RAtio of Pharmacokinetics (RAP)” is an absorbed dose of “with HL” converted using the representative RAP coefficient. (b) Same as (a) except that [^{211}At] MABG [6] is a reference. (c) Same as (a) except that [^{125}I]MIBG [7] is a reference. (d) Same as (a) except that [77Br]MBBG [7] is a reference.

Fig. 2 Inverse of the RAP coefficient at *t* (solid line) and the representative RAP coefficient (square) on [^{131}I]MIBG [5]. (a) Heart, liver, kidney, and intestine. (b) Blood, adrenals and stomach, and tumor tissue.

Fig. 3 Behavior maps of an optimal timing (solid line) on ^{211}At-labeled target compounds. T_{pA1} and T_{bA1} are the physical HL and HL of the biological clearance of a target, respectively. T_{bA2} is the half-life of the biological clearance of a reference. Behavior maps of T_{bA2} in these cases of 5, 10, 15, 20, 25, and 50 h are presented in the panels of (a), (b), (c), (d), (e), and (f), respectively. The dashed and dotted lines represent optimal timing in the cases of 0.95 and 1.05, and 0.9 and 1.1 times converted absorbed doses, respectively.

Fig. 4 Behavior maps of optimal timing (solid line) on radiolabeled target compounds with a physical HL of 10 d. T_{pA1} and T_{bA1} are the physical HL and HL of the biological clearance of a target, respectively. T_{bA2} is the half-life of the biological clearance of a reference. Behavior maps of T_{bA2} in these cases of 25, 50, 100, and 200 h are presented in the panels of (a), (b), (c), and (d), respectively. The dashed and dotted lines represent optimal timing in the cases of 0.95 and 1.05, and 0.9 and 1.1 times converted absorbed doses, respectively.

Fig. 5 Behavior maps of an optimal timing (solid line) on radiolabeled target compounds with a physical HL of 10 d. T_{pA1} and T_{bA1} are the physical HL and HL of the biological clearance of a target, respectively. (a) HL of the biological clearance of a reference, T_{bA2}, of 25 h. (b) HL of the biological clearance of a reference, T_{bA2}, of 1 h. The dashed and

dotted lines represent optimal timing in the cases of 0.95 and 1.05, and 0.9 and 1.1 times converted absorbed doses, respectively.

Fig. 6 Example of a RAP dose conversion using an optimal timing behavior map for a single biodistribution measurement (%ID/g) on ^{211}At-labeled target compounds. First, (a) plotted values converted to logarithms of [^{131}I]MIBG [5] corrected by the physical half-life of ^{131}I, i.e., a biological component, and fitted by the linear function (the dashed line). Second, (b) draws the behavior map of an optimal timing (solid line) on a target compound with a physical HL of 7.2 h and a reference with a 6.9 h HL of biological clearance, T_{bA2}, which was derived from the fitting curve on panel (a). The dashed and dotted lines represent optimal timing in the cases of 0.95 and 1.05, and 0.9 and 1.1 times converted absorbed doses, respectively. Finally, (c) converted absorbed doses of [^{131}I]MIBG [5], “with HL”, “with HL + RAP”, and a true target absorbed dose of [^{211}At]MABG [5].

Figures

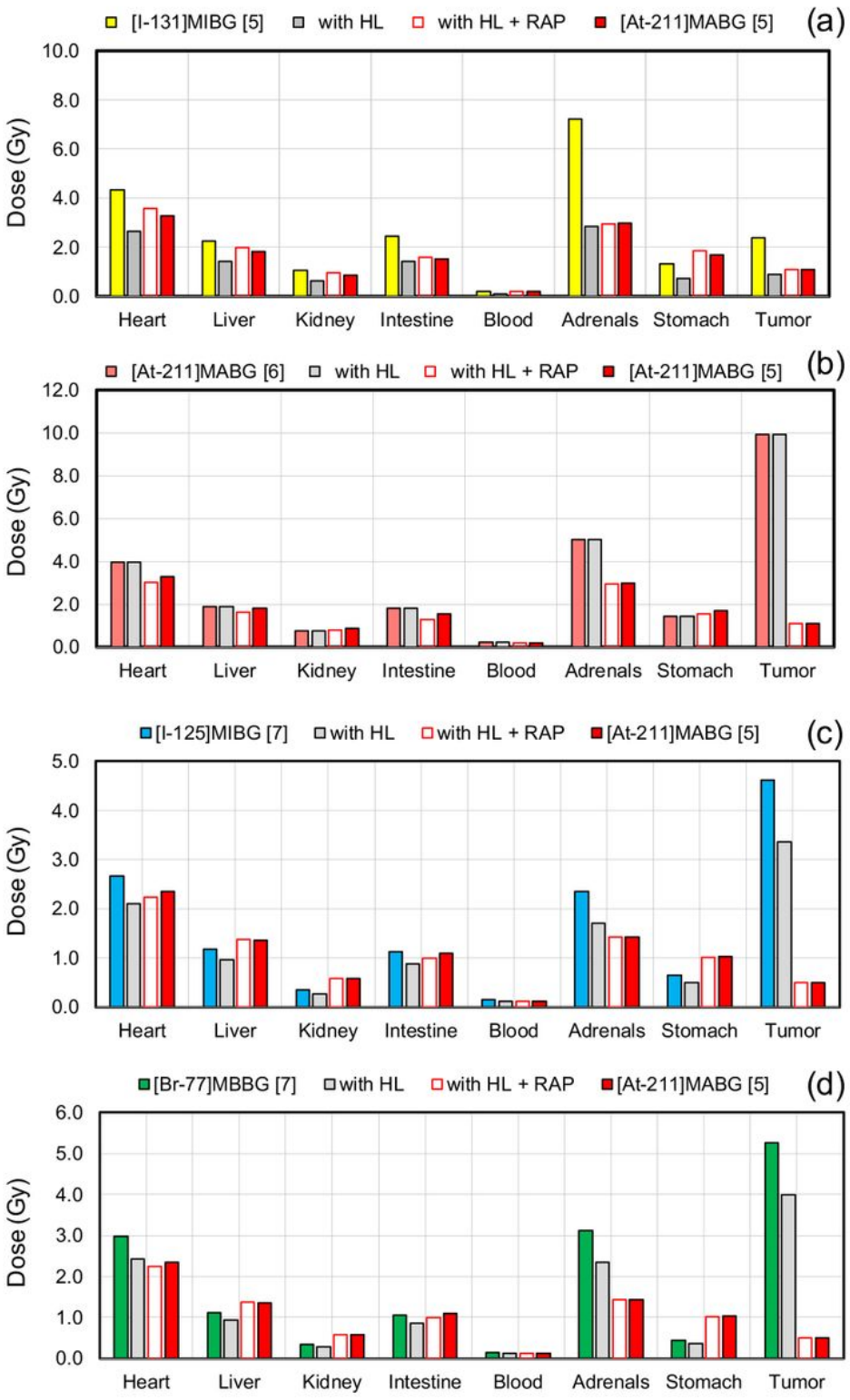

Figure 1

Comparison between converted absorbed doses of [131I]MIBG [5], [211At]MABG [6], [125I]MIBG [7], and [77Br]MBBG [7] and the true target absorbed dose of [211At]MABG [5]. (a) Converted absorbed doses from [131I]MIBG [5] as a reference, and absorbed dose of [211At]MABG [5] as a true target. [131I]MIBG [5]

indicates the absorbed dose of an organ or tumor tissue when alpha rays derived from 211At were emitted by the number of radioactive decays of 131I. “with half-life (HL)” shows a converted absorbed dose of [131I]MIBG [5] corrected by the physical half-life of 131I and radioactively decayed with the physical half-life of 211At, indicating the physical part of equation (5).“with HL + RAtio of Pharmacokinetics (RAP)” is an absorbed dose of “with HL” converted using the representative RAP coefficient. (b) Same as (a) except that [211At] MABG [6] is a reference. (c) Same as (a) except that [125I]MIBG [7] is a reference. (d) Same as (a) except that [77Br]MBBG [7] is a reference.

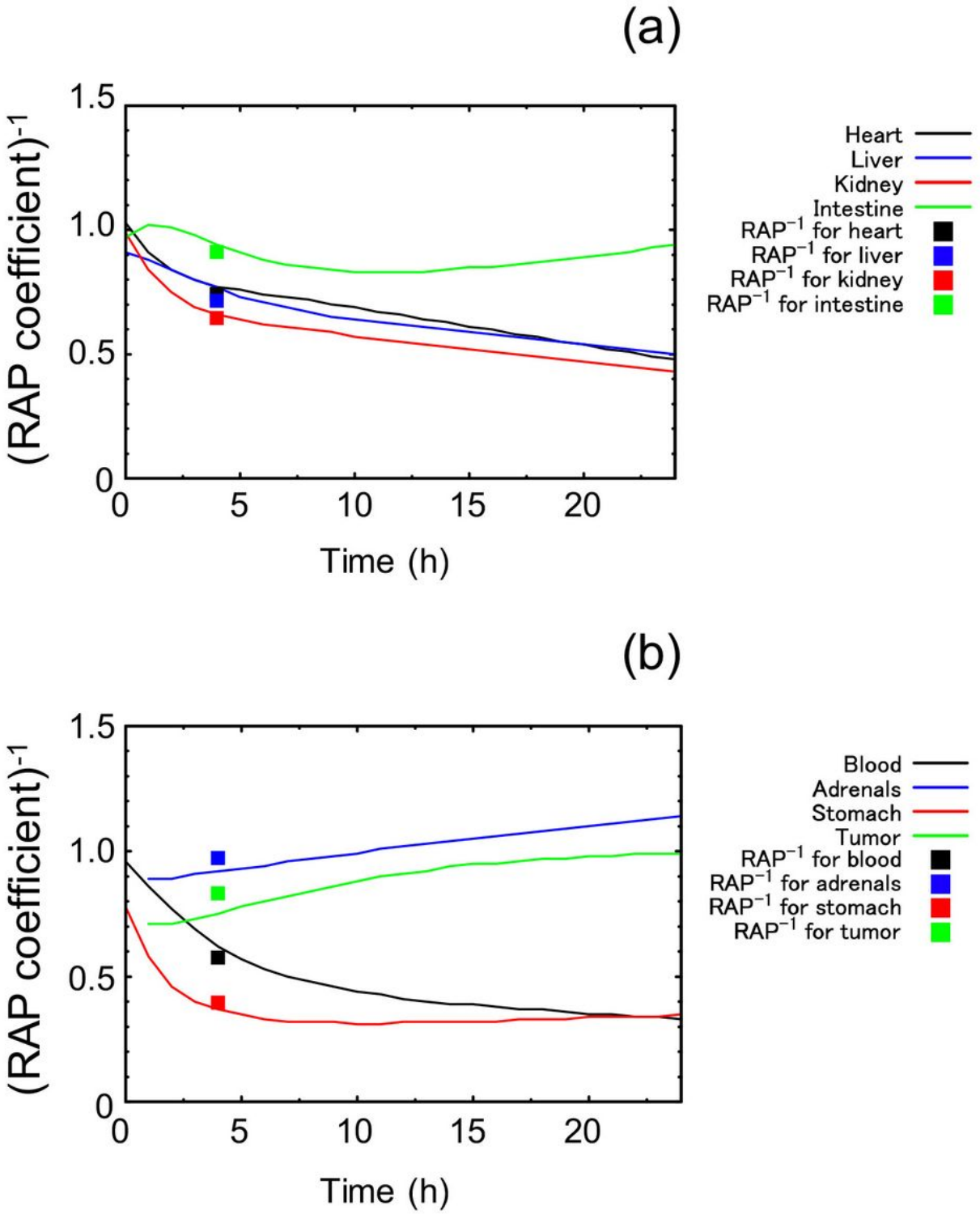

Figure 2

Inverse of the RAP coefficient at t (solid line) and the representative RAP coefficient (square) on [131I]MIBG [5]. (a) Heart, liver, kidney, and intestine. (b) Blood, adrenals and stomach, and tumor tissue.

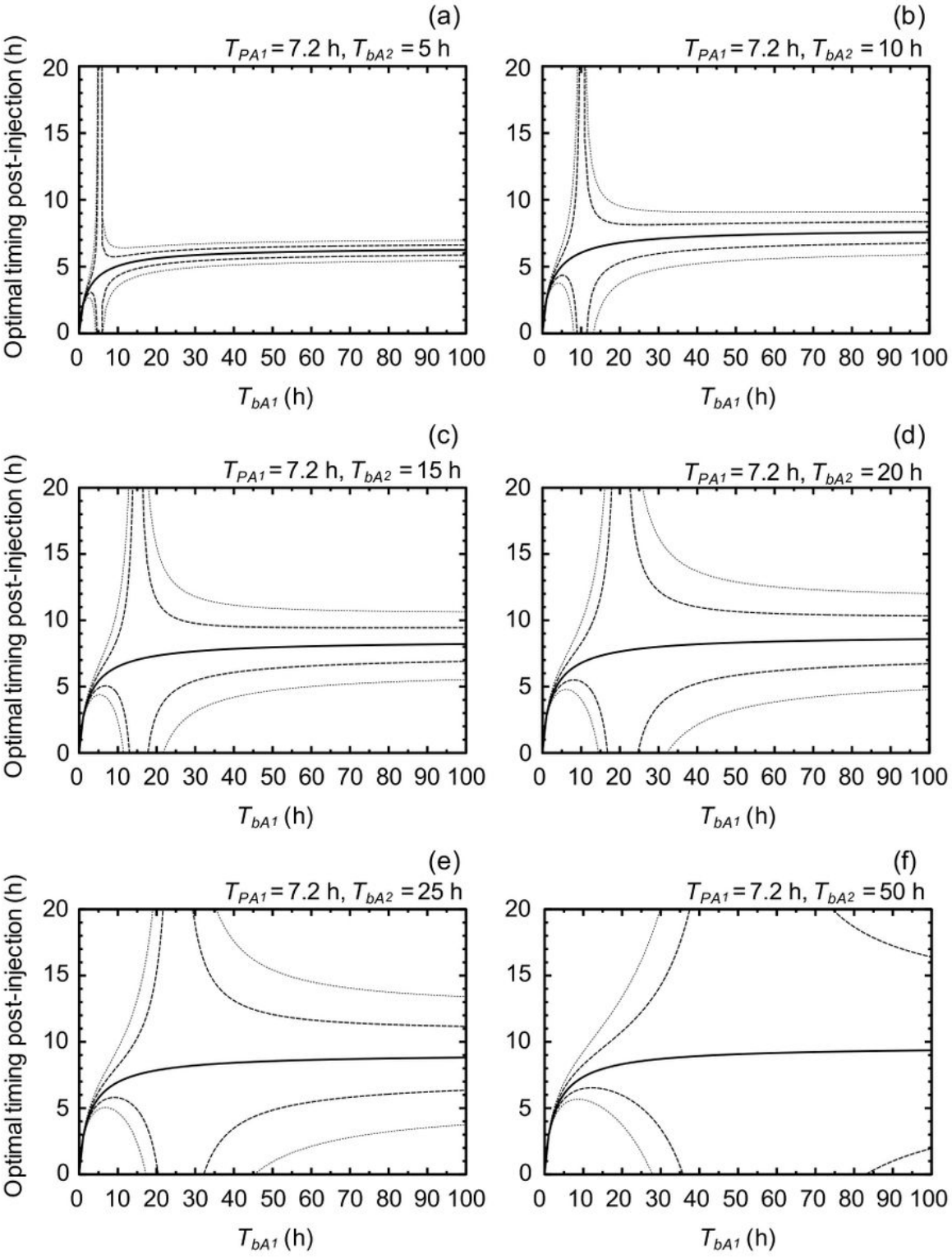

Figure 3

Behavior maps of an optimal timing (solid line) on 211At-labeled target compounds. TpA1 and TbA1 are the physical HL and HL of the biological clearance of a target, respectively. TbA2 is the half-life of the biological clearance of a reference. Behavior maps of TbA2 in these cases of 5, 10, 15, 20, 25, and 50 h are presented in the panels of (a), (b), (c), (d), (e), and (f), respectively. The dashed and dotted lines represent optimal timing in the cases of 0.95 and 1.05, and 0.9 and 1.1 times converted absorbed doses, respectively.

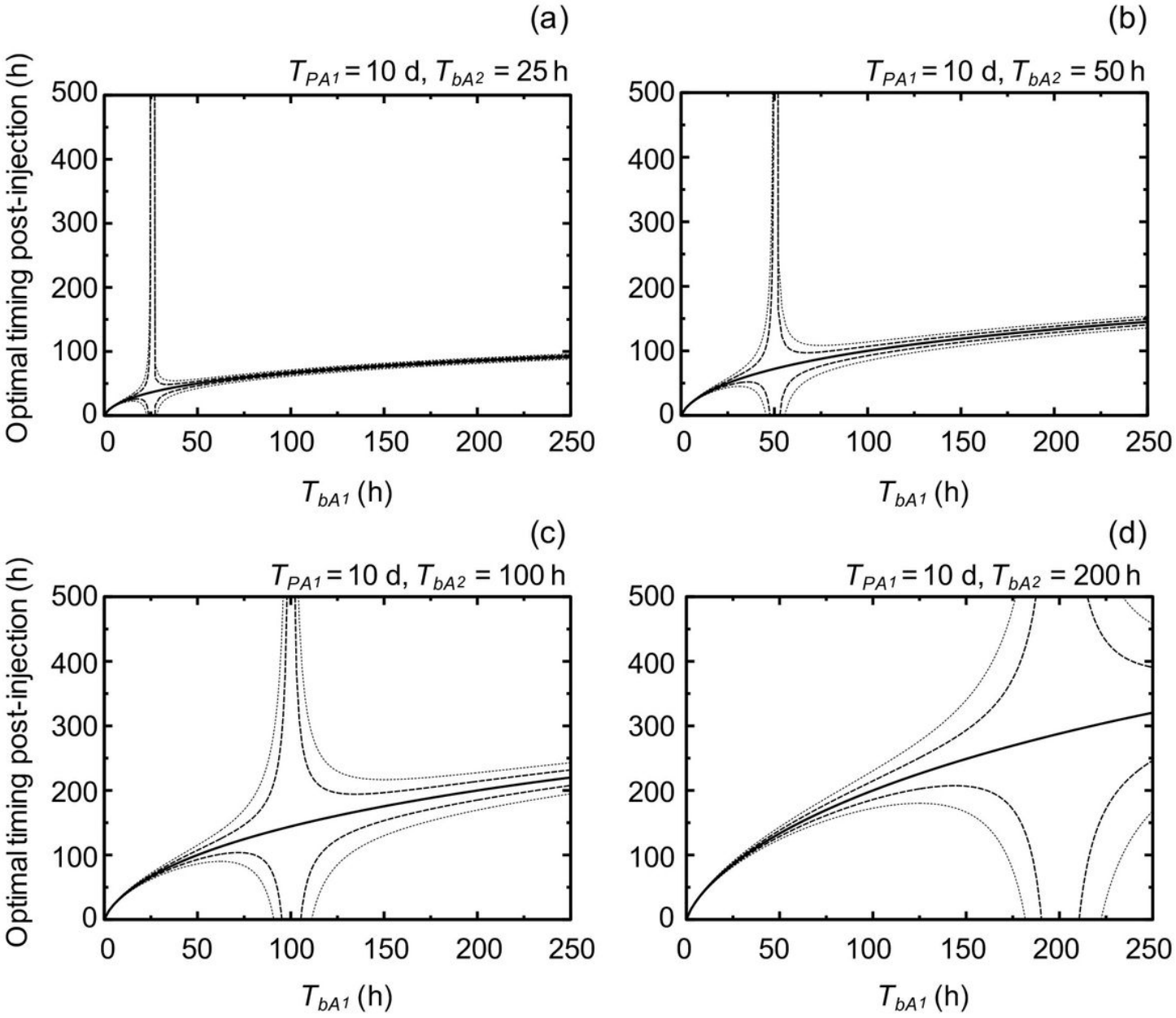

Figure 4

Behavior maps of optimal timing (solid line) on radiolabeled target compounds with a physical HL of 10 d. TpA1 and TbA1 are the physical HL and HL of the biological clearance of a target, respectively. TbA2 is the half-life of the biological clearance of a reference. Behavior maps of TbA2 in these cases of 25, 50, 100, and 200 h are presented in the panels of (a), (b), (c), and (d), respectively. The dashed and dotted

lines represent optimal timing in the cases of 0.95 and 1.05, and 0.9 and 1.1 times converted absorbed doses, respectively.

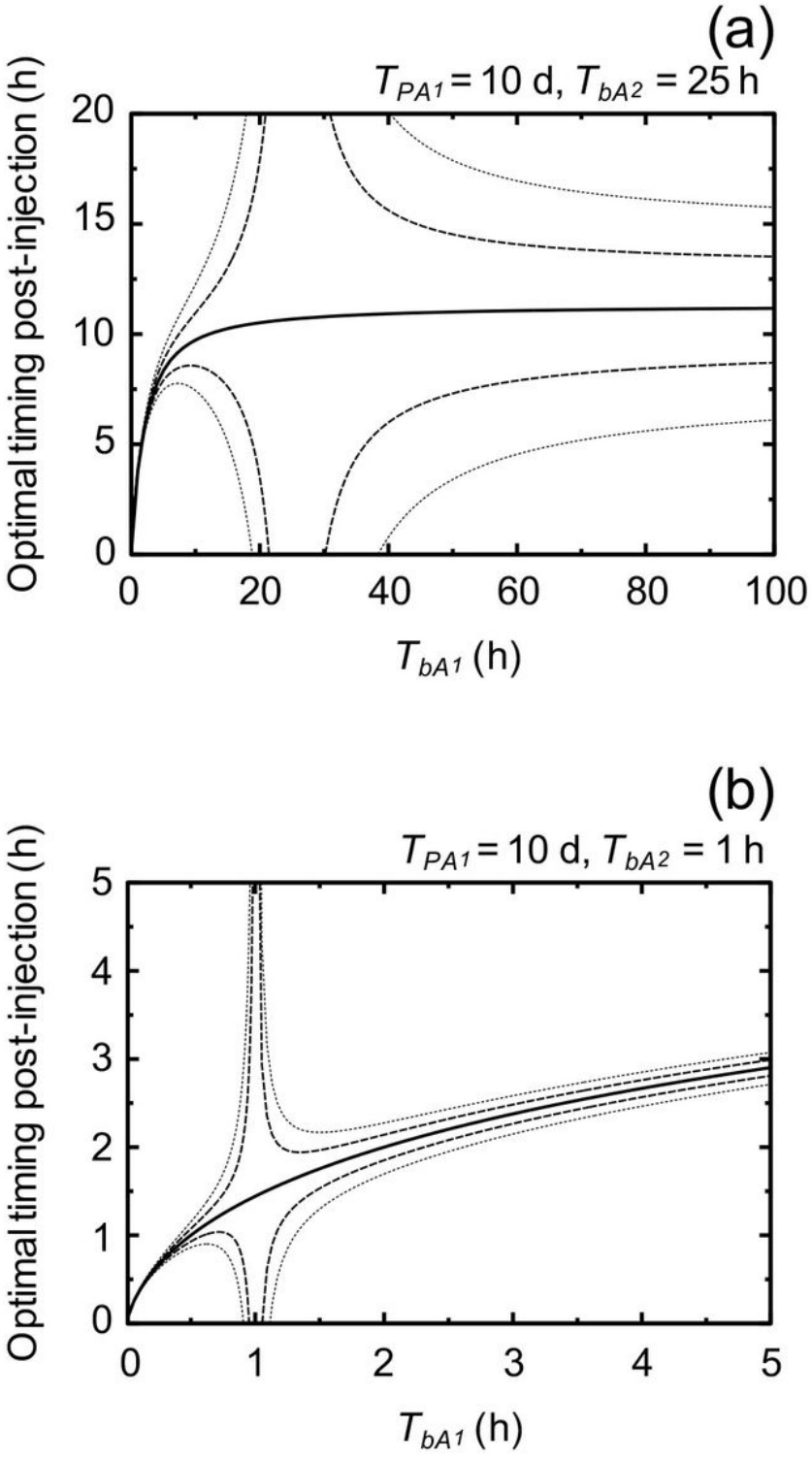

Figure 5

Behavior maps of an optimal timing (solid line) on radiolabeled target compounds with a physical HL of 10 d. TpA1 and TbA1 are the physical HL and HL of the biological clearance of a target, respectively. (a) HL of the biological clearance of a reference, TbA2, of 25 h. (b) HL of the biological clearance of a

reference, TbA2, of 1 h. The dashed and dotted lines represent optimal timing in the cases of 0.95 and 1.05, and 0.9 and 1.1 times converted absorbed doses, respectively.

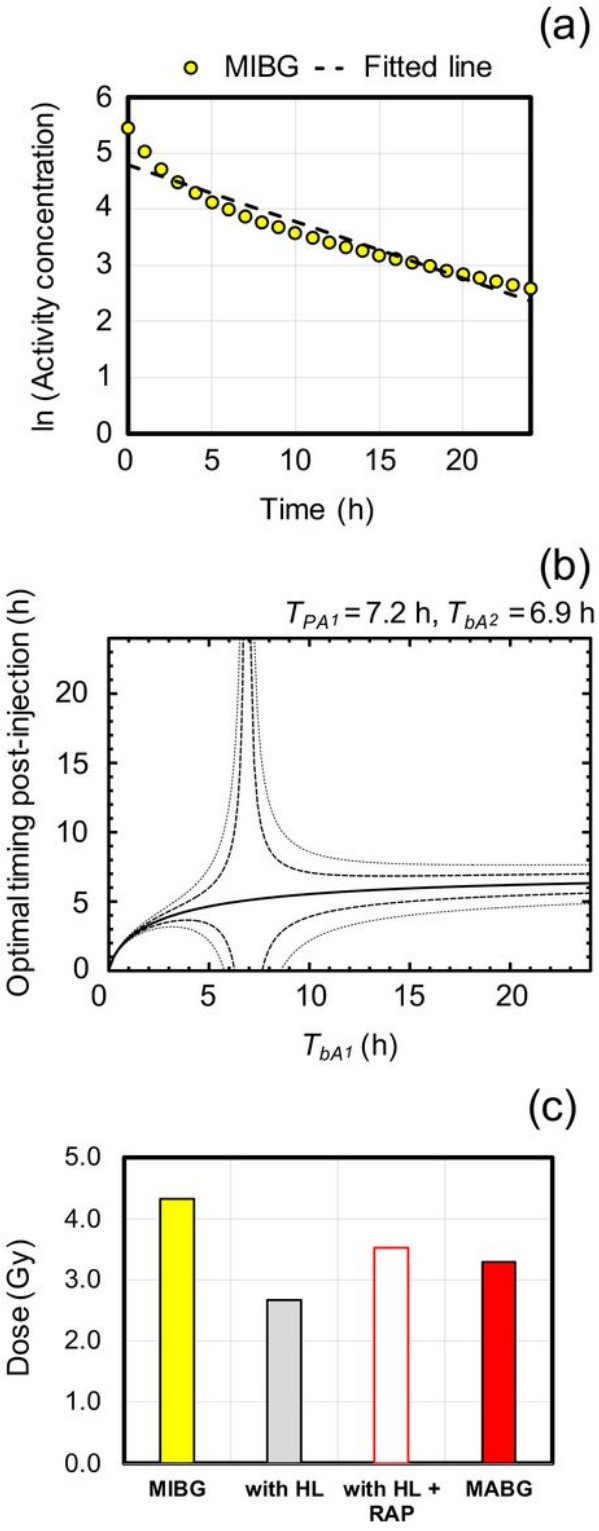

Figure 6

Example of a RAP dose conversion using an optimal timing behavior map for a single biodistribution measurement (%ID/g) on 211At-labeled target compounds. First, (a) plotted values converted to logarithms of [131I]MIBG [5] corrected by the physical half-life of 131I, i.e., a biological component, and

fitted by the linear function (the dashed line). Second, (b) draws the behavior map of an optimal timing (solid line) on a target compound with a physical HL of 7.2 h and a reference with a 6.9 h HL of biological clearance, TbA2, which was derived from the fitting curve on panel (a). The dashed and dotted lines represent optimal timing in the cases of 0.95 and 1.05, and 0.9 and 1.1 times converted absorbed doses, respectively. Finally, (c) converted absorbed doses of [131I]MIBG [5], “with HL”, “with HL + RAP”, and a true target absorbed dose of [211At]MABG [5].